ChemPubSoc Europe

DOI: 10.1002/ejic.201700182

EurJIC European Journal of Inorganic Chemistry

Full Paper

Noble-Metal Extraction

Synergistic Effect in Green Extraction of Noble Metals and Its Consequences

Abhijit Nag,[a][‡] Ananya Baksi,[a][‡] K. C. Krishnapriya,[a] Soujit Sen Gupta,[a] Biswajit Mondal,[a] Papri Chakraborty,[a] and Thalappil Pradeep*[a]

Abstract: Extraction of silver into water occurs from its apparently inert metal surface by the simple carbohydrate glucose. Here we show that there are large synergistic effects in the extraction process, which results in ca. 45 times larger leaching with specific molecules, when used along with glucose. While glucose (1 g) alone can extract ca. 650 ppb of silver from the metal, 60 mg of it extracts ca. 30000 ppb in a combination with 200 mg of glutathione (GSH) under similar experimental conditions of 70 °C and an extraction time of 7 d, in deionized (DI) water (200 mL). This enhancement is similar when glucose is replaced with cyclodextrin (CD). This enhanced concentration of silver in solution enables the formation of the silver clusters protected with glutathione and cyclodextrin, $Ag_{20}(SG)_{15}CD^{3-}$, in the presence of a reducing agent. A similar extraction for copper leads to excessive leaching, and typical concentrations are even higher than the solubility limit of the copper–glutathione complex. As a result, these complexes are precipitated. This synergistic extraction is observed for zinc and stainless steel as well. Enhanced extraction is a result of the formation of complexes of metals with glutathione and the consequent leaching of the complex into solution as well as the stabilization of the complex by inclusion complexation with cyclodextrin. Enhanced leaching in the presence of glucose is mostly due to simultaneous complexation with glucose as well as glutathione. The science presented may be used for the green extraction of different metals and could be a new potential top-down approach for metal cluster synthesis. This may also be useful for green and sustained leaching of minerals into water to regulate its quality.

Introduction

Ultra-small noble-metal nanoparticles like gold, silver, platinum and copper are extensively used in modern industries due to their unique properties like chemical inertness, catalysis, electrical and thermal conductivity and biocompatibility. Precious noble metals are known to be extremely inert towards chemical leaching. All the known noble-metal extraction processes used in industries are environmentally not friendly as highly toxic chemicals such as cyanide are used and are often discarded directly contributing to the pollution of water and soil. It is necessary to have a green and efficient method to extract noble metals. On the other hand, such metal ions in solution are generally used to make nanoparticles with environmentally friendly reducing agents such as citric acid.[1] The new interest in this class of materials is in atomically precise clusters,[2] which can be obtained by tuning various synthetic parameters and appropriate protecting agents. Most of the solution-based cluster-synthesis methods involve bottom-up approaches following the modified Brust synthesis protocol.[3] Direct synthesis of such nanomaterials from the metallic state requires strong interaction of the metal with specific molecules, resulting in the extraction of the metal in solution. This is often done with ions such as cyanide, which form strong complexes with noble metals. Biomolecules such as proteins, lipids and carbohydrates are known to form weak non-covalent complexes with several metals.[4] Square-planar tetrahaloaurate anions ($[AuX_4]^-$, X = Cl/Br) form inclusion complexes with α-, β-, and γ-CDs.[5] A strong affinity of the functional groups such as –OH, $–NH_2$, –COOH, –SH, etc., towards metals including gold and silver attracted researchers to create novel nano-biocomposites involving such functionalities.[3k,6] However, such interactions are rarely used for the extraction from the bulk metal in industry due to poor efficiency. There are a few reports where metals are first extracted into the biological system as ions/complexes and small nanoparticles are synthesized in vivo, mostly within the bacterial cells, which follows the biomineralization pathway.[7] Electrochemical dissolution of the noble metals is an important method for extracting, refining and processing this metal to its compounds.[8] Baksi et al. have recently reported the extraction of silver into solution from the bulk metal by carbohydrates, mainly glucose.[9] By modifying certain experimental conditions they could grow plasmonic nanoparticles with the extracted ionic silver. This observation opened up a new possibility of creating new materials directly from the metallic state using suitable ligands that show a relatively stronger affinity to a specific metal.

[a] *DST Unit of Nanoscience (DST UNS) and Thematic Unit of Excellence, Department of Chemistry, Indian Institute of Technology Madras, Chennai 600036, India*
E-mail: pradeep@iitm.ac.in
http://www.dstuns.iitm.ac.in/pradeep-research-group.php
[‡] These authors contributed equally to this work.
Supporting information for this article is available on the WWW under https://doi.org/10.1002/ejic.201700182.

In this paper, we show large synergistic effects in the green extraction process of glucose, which results in the enhancement of leaching by about 45 times with specific molecules. About 30 ppm of silver can be extracted by glucose (60 mg) and glutathione (200 mg) after 7 d of incubation in DI water (200 mL). We show a direct approach to synthesize silver clusters from metallic silver by dissolution of the metal in solution in the presence of carbohydrates and glutathione and subsequent reduction by sodium borohydride. Under these conditions we created a new cluster, $Ag_{20}(SG)_{15}CD^{3-}$ [CD: γ-cyclodextrin; SG: glutathione thiolate (GSH–H)]. Cluster formation is dependent on the amount of silver leached into the aqueous medium, which in turn depends on the nature of the carbohydrate used as well as the complexing agent. Highly polished silver foil as a silver source, glucose and β- and γ-cyclodextrin as the carbohydrate sources, and glutathione and mercaptobenzoic acid as complexing agents were used in this study. A detailed time- and quantity-dependent study was performed, and the product was continuously monitored by several spectroscopic and mass spectrometric techniques. The surface of the silver foil was studied in detail by different microscopic and spectroscopic techniques. The roughened silver foil surface acts as an effective substrate for surface enhanced Raman spectroscopy (SERS).

Results and Discussion

For the first set of experiments, the reactions were carried out for 7 d by immersing 3 g of silver foil (6 cm × 6 cm) in a solution containing glucose (60 mg) and GSH (200 mg), in DI water (200 mL), at 70 °C, in a teflon beaker. Under these specific conditions, a maximum of 30 ppm of silver was found in the solution (Table 1) after 7 d. In comparison, 1 g of glucose alone can extract only 656 ppb of silver into solution under the above-mentioned conditions (Table 1). An enhancement of 45 times in the process of extraction was found. The large synergistic effects could be explained by ITC measurements. The free energy (ΔG) of the reaction of the $AgNO_3$ vs. GSH/glucose mixture was more negative compared to the reaction with glucose alone. The rate constant was found to be 1.14×10^5 M^{-1} for the mixed system, whereas for glucose only, it was 304 M^{-1} (Figures S1 and S2). Peptides containing cysteine residues are known to show a strong interaction towards noble metals. Glutathione is known to form complexes with silver and gold and also act as ligands in their clusters.[9,10] γ-CD is also a carbohydrate like glucose. When glucose was replaced by γ-CD keeping all the other parameters the same, maximum silver leaching was 26.4 ppm (Table 1) with the combination of 60 mg of γ-CD and 200 mg of GSH, whereas for 1 g of γ-CD only 120 ppb of silver was detected (see Table 1). Under these conditions, extracted silver forms a stable complex with GSH as well as with glucose/γ-CD. The Ag complexes formed in this process were characterized using ESI MS (Electrospray Ionization Mass Spectrometry). The ESI mass spectra were recorded as a function of time, typically on a daily basis [Figures S3(C) and S3(D)]. Different silver complexes were observed [Figure 1(A)] in the presence of glucose and glutathione as $Ag_2G(SG)Na^+$ (m/z = 723), $Ag_2G(SG)_2Na^+$ (m/z = 922), $Ag_2G(SG)_2Na^+$ (m/z = 1029), $Ag_2G_2(SG)_2Na^+$ (m/z = 1102), $Ag_4G(SG)_2^+$ (m/z = 1220), $Ag_4G_2(SG)_2^+$ (m/z = 1404), etc., as shown in Figure 1(A) and Figure S3(D), where G and SG refer to glucose and glutathione thiolate (GSH–H), respectively. When γ-CD was used in place of glucose, silver–glutathione–γ-CD complexes were found [Figure 1(B)].

Table 1. Silver extraction by glucose, glucose + GSH, γ-cyclodextrin and γ-cyclodextrin + GSH, as a function of time.

Time	Glucose [ppb]	Glucose + GSH [ppb]	γ-CD [ppb]	γ-CD + GSH [ppb]
Day 1	190	10644	42	10374
Day 2	209	15550	47	11219
Day 3	356	17156	75	12374
Day 4	398	18358	97	14383
Day 5	502	19621	99	18167
Day 6	578	23740	106	23557
Day 7	656	30019	120	26415

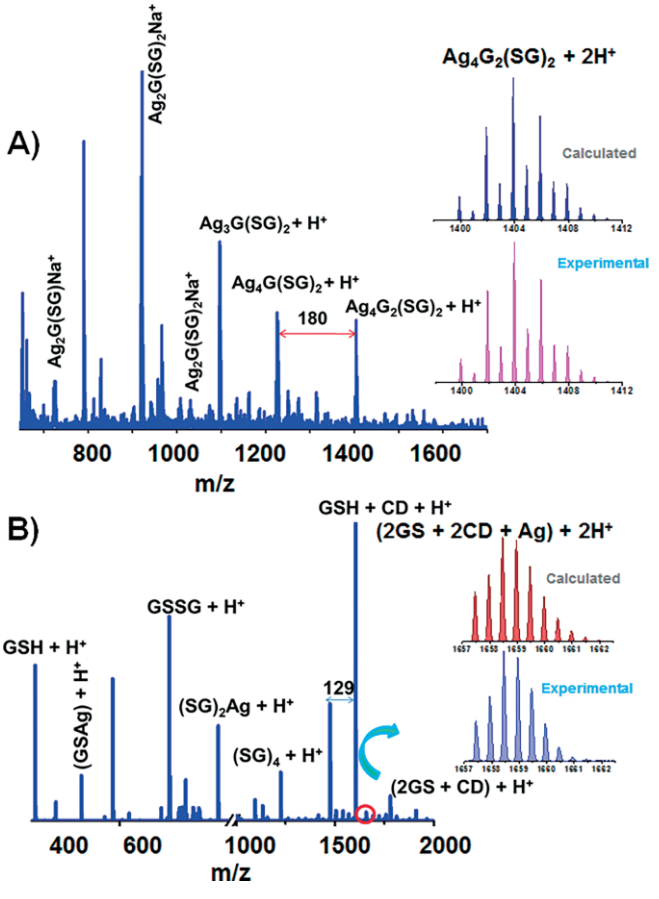

Figure 1. (A) ESI MS data for glucose/GSH mixture exposed to Ag foil. In the positive mode, ions such as $Ag_2G(SG)Na^+$ (m/z = 723), $Ag_2G(SG)_2Na^+$ (m/z = 922), $Ag_2G(SG)_2Na^+$ (m/z = 1029), $Ag_2G_2(SG)_2Na^+$ (m/z = 1102), $Ag_4G(SG)_2^+$ (m/z = 1220), $Ag_4G_2(SG)_2^+$ (m/z = 1404) were found. (B) ESI MS data from the γ-CD/GSH reaction mixture exposed to Ag foil.

The subsequent studies were carried out with cyclodextrin and glucose for the extraction of different metals. About 70 mg of γ-CD was added to silver, copper, brass and stainless steel

vessels in DI water (70 mL). The reaction temperature was kept at 65 °C, while stirring for 7 d. After 7 d, all the solutions from these four vessels were analyzed by ICP MS (Inductively Coupled Plasma Mass Spectrometry) to evaluate the concentration of the different metals in the different vessels (Table 2).

Table 2. Concentration of possible metals from different vessels analyzed by ICP MS. All the experiments were carried out with 70 mg of γ-cyclodextrin in 70 mL of DI water at 65 °C for 7 d, and the final concentrations of different metals are listed in the table.

Metal	Steel vessel [ppb]	Copper vessel [ppb]	Brass vessel [ppb]	Silver vessel [ppb]
Ni	9	226	84	307
Cu	157	188300	9300	2840
Ag	1	4	2	545
Al	120	0	22	43
Mn	294	4	7	8
Fe	602	53	0	13
Zn	39	3000	50000	148
Cr	24	0	0	1
Co	1	623	2	43
V	0	0	0	0
Ti	0	0	1	2
Mo	0	0	2	0

To compare the ease of reactivity towards different metals, all the experimental conditions were kept the same. Uniform vessels of 100 mL were chosen for the experiments and were procured from the local market. The individual vessels contained > 91 % of the specified metal. All possible metal concentrations were analyzed by ICP MS and are listed in Table 2. Although there are variations in composition, there is still a clear preference of γ-cyclodextrin towards copper and zinc over silver and iron. The brass vessel is composed of 60.66 % copper, 36.58 % zinc with small amounts of iron and tin. Extracted copper and zinc do not follow their original ratio as the zinc concentration is far higher than the copper one confirming the preference for zinc over copper when both are present in adequate amounts. Similarly, the silver vessel used in our study contained about 1.5 % Cu (w/w), but the copper concentration in the solution is higher than that of Ag, which again confirms preferential extraction of Cu in the presence of Ag. The reason could be the solubility of the individual complex in water and the tendency of the metal ion to form inclusion complexes with γ-cyclodextrin. Similar types of reactions were performed with glucose (70 mg of glucose in 70 mL of DI water) instead of γ-CD (Table S1), which also follows a similar trend. This indicates that the initial solubility of the ion/complex in the solution plays a major role in the extraction. As more and more metal ions interact with glucose or cyclodextrin, more extraction is observed in the solution.

Figure 2(A) shows a schematic of two stages of the reaction on the metal surface where activated metal ions are extracted, which formed effective complexes with cyclodextrin.[11] ESI MS was performed to identify the molecular-level interactions at each concentration. Species such as $(\gamma\text{-CD} + Ag)^+$, $(\gamma\text{-CD} + Zn + \gamma\text{-CD})^{2+}$ and $(\gamma\text{-CD} + Cu + \gamma\text{-CD})^{2+}$ were detected by ESI MS in the positive ion mode from silver, brass and copper vessels, respectively [see Figure 2(B), (C) and (D) (i)]. For the above species, the calculated spectra matched the experimental ones [see Figure 2(B), (C) and (D) (ii)]. The extended species appear to be Ag^+, Zn^{2+} and Cu^{2+}, which are complexed with the neutral molecular species. For the subsequent studies, we have focused mostly on silver and copper. The silver vessel was replaced by silver foil to better understand the surface using direct analysis techniques. Several control experiments were carried out with varying amounts of glutathione without altering the amount of γ-CD and other parameters in the solution to check the dependence of GSH amounts on silver extraction and cluster formation. The concentration of silver was monitored as a function of time (days) using ICP MS. Four sets of reactions were planned, they were: (i) 60 mg of γ-CD and 50 mg of GSH, (ii) 60 mg of γ-CD and 100 mg of GSH, (iii) 60 mg of γ-CD and 150 mg of GSH and (iv) 60 mg of γ-CD and 200 mg of GSH (from a 1:4 to 1:16 molar ratio for γ-CD/GSH). High amounts of silver were extracted by these processes. In the case of (i) and (ii), 9.30 and 15.77 ppm of silver, respectively, were observed in the solution after 5 d [Figure S4(A) and (B)]. In the case of (iii) and (iv), 16.98 and 18.16 ppm of Ag were extracted after 5 d [Figure S4(C) and (D)]. Upon increasing the amounts of GSH, the silver concentration increases in the solution. After 2 d of continuous heating, the colour of the solution turned from colourless to light yellow. This is mainly because of the complexation of incoming silver ion with glucose/γ-CD and GSH in the solution to form mixed silver thiolate (and individual complexes), which has a pale yellow colour. The colour deepens with time as the concentration of silver increases in the solution. After 5 d, the colour and texture of the silver foil had changed visibly. Plausibly, excess glutathione was adsorbed on the metal foil. For the cluster synthesis, we proceeded with 60 mg of γ-CD and 200 mg of GSH as more amounts of silver were etched by this method. These solutions were used as precursors for cluster formation. About 400 μL of ice-cold $NaBH_4$ (1 M) solution was added to the extracted silver solution (3 mL) to reduce the thiolates formed. The colour change was not prominent when the silver concentration was not high enough (ca. 10 ppm). With a slightly higher silver concentration (ca. 12 ppm), a brownish colour was observed, which was not stable. The colour disappeared immediately on shaking but reappeared after a few minutes. This suggested the formation of metastable intermediates. It was reversible and was seen many times. At a higher silver concentration (14 ppm and higher), a persistent brown cluster was found, which was stable for 2 h. UV/Vis spectra were recorded for all the solutions. The spectra revealed thiolate/nanoparticle/cluster formation [Figure S5(A)]. For 50 mg of GSH and 60 mg of γ-CD solution, thiolate was detected with its characteristic peak at 370 nm. It was comparable to the previously reported peaks of thiolates.[12] A peak at 414 nm from the plasmonic nanoparticles was observed when 100 mg of GSH was used. With higher amounts of GSH (150 and 200 mg), a peak at 457 nm was seen that intensified with time as the silver concentration increased [Figure S5(D)]. A similar absorption peak was seen previously for glutathione-protected silver clusters.[10b,13] Note that with increasing amounts of the protecting agent, the core size of the particles decreases. A parallel reaction was performed with glucose (60 mg) instead

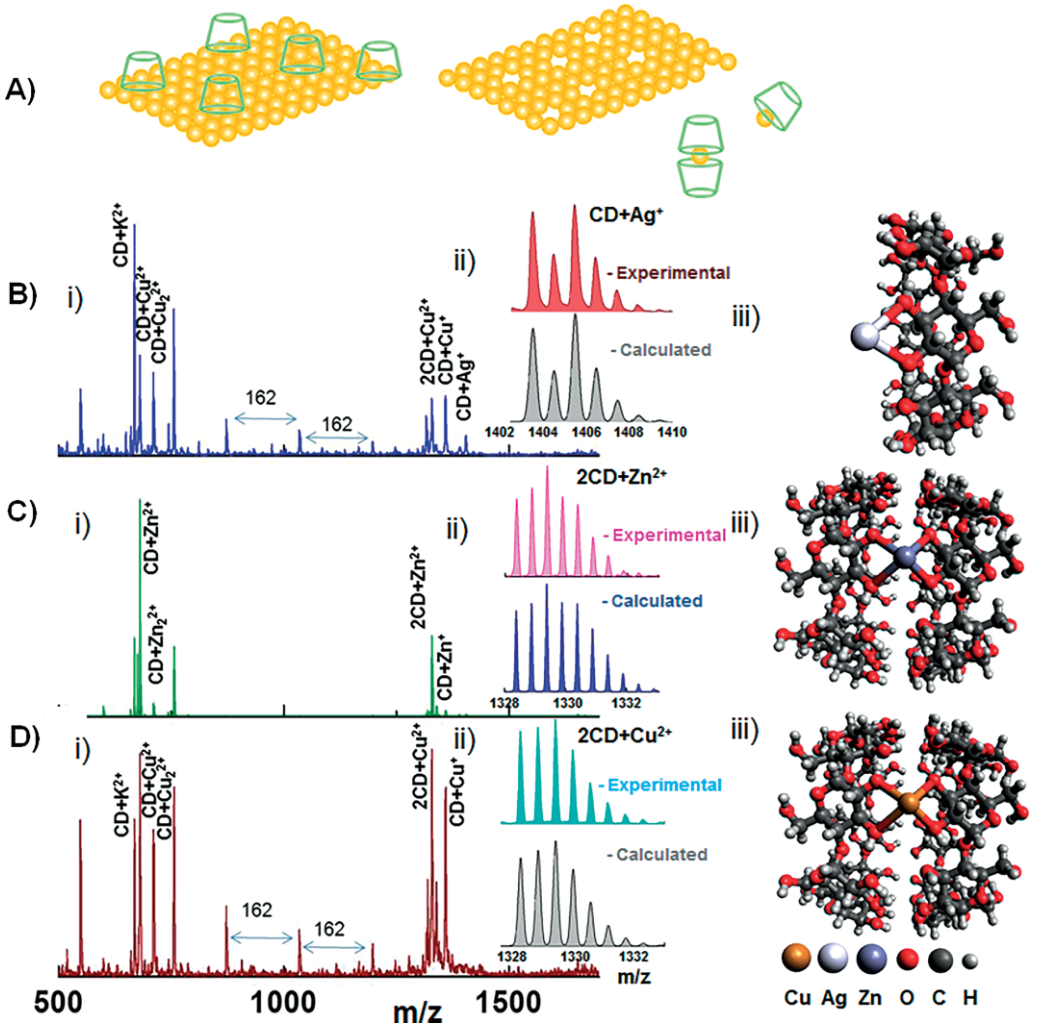

Figure 2. (A) Schematic representation of the silver extraction by a γ-CD solution. The interaction of γ-CD with the metal surface is shown. (B) (i), (C) (i) and (D) (i) are the ESI mass spectra of the solutions from the silver, brass and copper vessels, respectively. (B) (ii), (C) (ii) and (D) (ii) are the theoretical and experimental mass spectra of the inclusion complexes, $(\gamma\text{-CD} + Ag)^+$, $(\gamma\text{-CD} + Zn + \gamma\text{-CD})^{2+}$ and $(\gamma\text{-CD} + Cu + \gamma\text{-CD})^{2+}$, respectively. (B) (iii), (C) (iii) and (D) (iii) are the schematic representations of the $(\gamma\text{-CD} + Ag)^+$, $(\gamma\text{-CD} + Zn + \gamma\text{-CD})^{2+}$ and $(\gamma\text{-CD} + Cu + \gamma\text{-CD})^{2+}$ structures, respectively.

of γ-CD where the absorption maximum was found to be 453 nm [Figure S5(C)].

Mass Spectrometric Understanding

The as-synthesized cluster was characterized by ESI MS. A 1:1 MeOH/H_2O (v/v) mixture was used as the solvent without further purification. A negative ion ESI MS is shown in Figure 3(B) where two distinct envelopes were observed in the mass range of m/z = 1750–2000 and 2680–2710 with a distinct separation between the neighbouring peaks. Optimized conditions are given in the Experimental Section. The effect of each and every parameter on the mass spectrum was thoroughly examined such as flow rate, capillary voltage and capillary temperature. The peak between m/z = 2680 and 2710 is a triply charged species, and the peak between m/z = 1750 and 2000 is a quadruply charged species. We have assigned the cluster as $Ag_{20}(SG)_{15}CD^{3-}$ [Figure 3(B)]. The theoretical mass spectrum of the cluster with a 3– charge state is shown in Figure 3(B) (ii) and matches well with the experimentally observed one. Multiple Na attachments are possible with GSH due to the presence of two –COOH groups in it. Such attachments were observed in Ag clusters before.[12,13] There is a report that CD stabilizes ligand-protected noble-metal clusters.[14] In our case, CD stabilizes the silver clusters in addition to enhancing extraction, as it forms an inclusion complex with GSH. In the ESI mass spectra other peaks like CD^-, CD_2^-, $(CD + SG)^-$ and $(CD + E)^-$ were observed in the negative ion mode.

Electron Microscopy and Spectroscopic Studies

The surface of the silver foil is modified upon extraction of silver in solution as seen in the previous study. The reacted silver foil was further investigated by SEM/EDS where the presence of Ag and S was confirmed [Figure S6(A)]. Elemental mapping of the same showed a uniform distribution of Ag and S on the surface suggesting strong adsorption of GSH on the silver surface. Note that the silver foil was washed repeatedly after the experiment

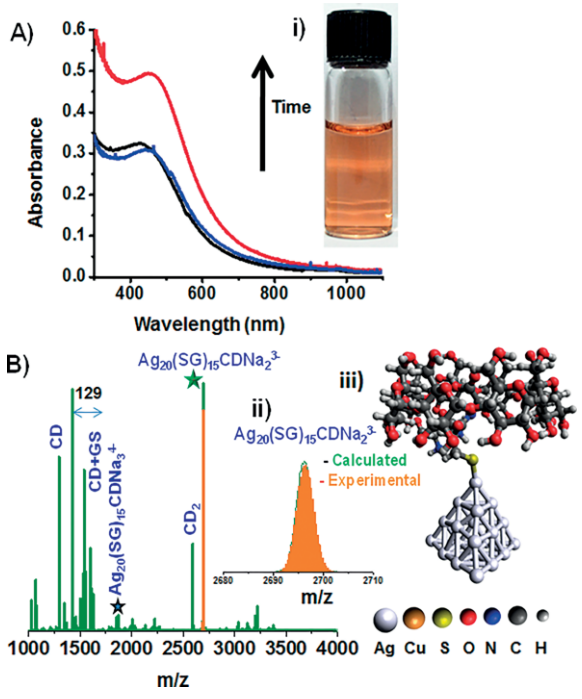

Figure 3. (A) Time-dependent UV/Vis absorption spectra of the cluster in the presence of γ-CD and GSH showing increased absorption at 457 nm with time. For plasmonic silver nanoparticles, the shape and peak maxima are different. (A) (i) Photograph of the cluster solution. (B) ESI MS of the clusters in the negative ion mode showing 3– and 4– species along with other peaks. Theoretical mass spectrum of the cluster of a specific charge state, which matches well with the experimentally observed one as shown in (B) (ii). Note that the isotope distribution is wide, as this is a metal cluster. (B) (iii) is a schematic representation of the cluster. Only one ligand is shown, which forms an inclusion complex with CD.

with water to get rid of excess ligands sticking to the surface. The presence of these species was further proved by Raman spectroscopy where characteristic peaks of both γ-CD and GSH were observed from the silver foil [Figure S6(B)]. In the case of pure glutathione, peaks at 2942, 2520 and 482 cm^{-1} correspond to the C–H symmetric, S–H symmetric and C–C symmetric stretching modes, respectively. A shift of a few cm^{-1} was observed for the C–H and S–H symmetric stretching modes of GSH as it adsorbed onto the silver surface.[15]

To check the dependence of the phenomenon of extraction on the complexing ligand, another water-soluble ligand, MBA, was used in this study instead of GSH. MBA was used before for synthesizing Au and Ag clusters, among which Au_{102}-(p-MBA)$_{44}$ and Ag_{44}(p-MBA)$_{30}$ are the most celebrated examples.[2m,16] Different control experiments were performed by varying the amounts of MBA and keeping all other conditions the same, such as (i) 50 mg of β-CD and 50 mg of MBA, (ii) 50 mg of β-CD and 75 mg of MBA, (iii) 50 mg of γ-CD and 50 mg of MBA, (iv) 50 mg of γ-CD and 75 mg of MBA and (v) 60 mg of MBA alone; all in 200 mL of DI water. Clusters were synthesized according to the same procedure as that discussed in the case of GSH. For both β-CD and γ-CD, absorption features of the synthesized clusters were the same except for the slight redshift (8 nm) in the case of γ-CD as shown in Figures S7(A) and (B). In the presence of only MBA, silver extraction was less, and the thiolate was reduced to nanoparticles instead of clusters. The data are presented in Figure S7(C). Blade-like structures with sharp edges were seen when the reacted silver foil was observed under the SEM [Figure 4(A) and (B)]. To further investigate these structures, TEM images were taken after dispersing the material in DI water [Figure 4(C) and (D)]. Blade-like sharp edges were also observed in the TEM images. In EDS the ratio of Ag/S was found to be 1:1 and 1:2 (Figure S9) when different positions were scanned. To confirm that these were silver thiolates, powder XRD was performed on the same material after dispersing it in DI water [Figure 4(G)]. From the powder XRD patterns, two types of silver thiolates were found. Their structures are given in Figure 4(F), which was also supported by TEM/EDS data. Prominent (00l) and (0l0) reflections suggest layered structures, which are characteristic of thiolates. These explain the blade-like morphology. This supports the strong adsorption capacity of MBA on the silver surface. This was further proved by Raman spectroscopy where almost all features of MBA were seen [(Figure 4(E)]. The peak at 1102 cm^{-1} is attributed to the aromatic ring vibration, and the band at 1606 cm^{-1} is from the aromatic ring breathing mode.[17] The less intense band at 1381 cm^{-1} is the (COO–) stretching mode. Other weak bands at 1163 and 1204 cm^{-1} correspond to the C–H deformation modes, which all match with those of MBA. There were some shifts in the C–S stretching mode, which proved the adsorption of MBA onto the silver surface. The S–H stretching mode at 2562 cm^{-1} of MBA (red) was absent for the adsorbed MBA. Because of the nanostructured surface and high roughness, silver foil acts as a SERS substrate, which in turn is responsible for the signal enhancement.[18] The blade-like structure was not observed for GSH and the signal intensity was also weak. Reasons could be the solubility difference of the Ag–MBA and Ag–GSH complex in water since MBA is less soluble in water than GSH at neutral pH. Another reason could be the lower reactivity of GSH towards the silver foil compared to that of MBA.[2f] The strong thiolate overlayer reduces silver dissolution in the case of MBA.

To understand this preferential extraction of one metal over another, different sets of experiments were performed. An isothermal titration calorimetric study was performed with Cu^{2+}, Ag^{+} and Zn^{2+} with glucose to compare their complexation thermodynamics. Data suggest (Figure S1) that the affinity towards Cu^{2+} and Zn^{2+} is stronger than that of Ag^{+}, which is also reflected in their extraction. Between silver and copper, both glucose and γ-CD showed a higher affinity towards Cu^{2+} than Ag^{+}. To understand the mechanism of Cu extraction and further understand the possibility to create nanomaterials with the extracted Cu, detailed studies were performed using the Cu vessel. About 70 mg of glucose in 70 mL of DI water can extract 248 ppm of copper from the copper vessel (Table S1), whereas the same amounts of γ-CD (70 mg in 70 mL of DI water) can extract 188 ppm of copper under the above conditions (Table 2). To this copper-extracted solution, freshly prepared ice-cold $NaBH_4$ solution was added, and the colour of the mixture changed immediately to dark green, indicating the formation of Cu nanoparticles, which was confirmed by UV/Vis spectroscopy with its characteristic peak at 590 nm [Figure 5(A)].

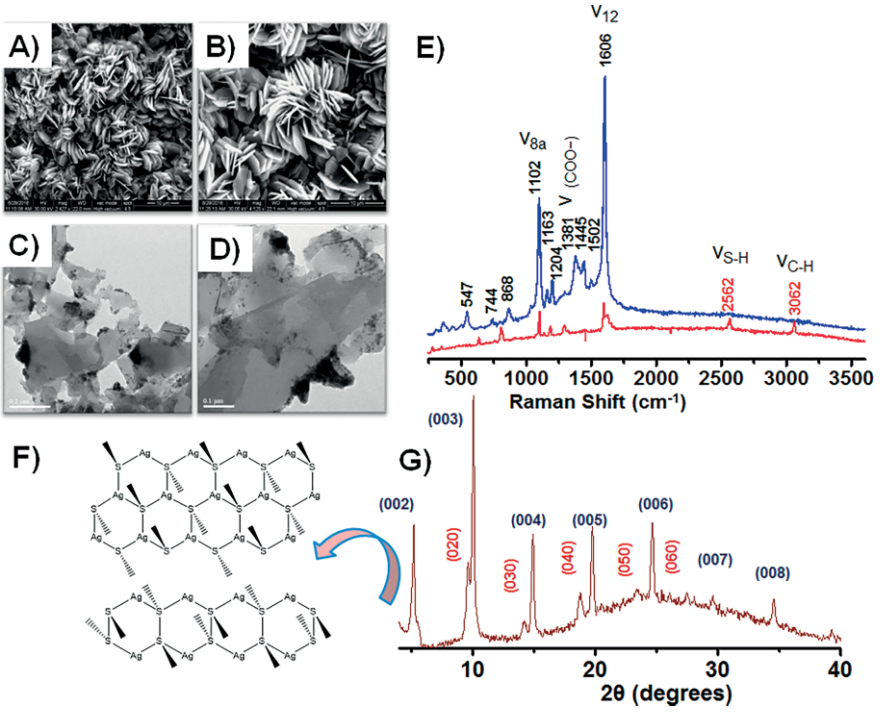

Figure 4. (A) and (B) SEM images of the reacted silver foil. Blade-like sharp structures were seen for the SEM. (C) and (D) TEM images of the same material after dispersion in DI water. (E) Raman spectra of the silver foil in the γ-CD + MBA solution (blue) and in MBA only (red). (G) Powder XRD of the same material after dispersion in DI water and (F) the corresponding silver thiolate structures.

The as-formed nanoparticles were almost uniform in size (5 nm) with the Cu (111) lattice seen in TEM [Figure 5(C)]. To find the enhancement in copper extraction using GSH, 50 mg of γ-CD and 100 mg of glutathione were placed in a copper vessel with 70 mL of DI water. The reaction mixture was kept at 65 °C while stirring for 2 d. The synergic effect of GSH and γ-CD resulted in excessive leaching and the as-formed blue complex was precipitated as the concentration was above the solubility of the copper–glutathione complex. To further understand the nature of the complex formed in this process, the solution was studied extensively using ESI MS [Figure 5(D)]. γ-CD is known to form complexes with GSH according to the host–guest mechanism. Both γ-CD and GSH are known to form complexes with Cu, and hence the resulting solution was expected to have all of these characteristic peaks in the ESI mass spectra. Along with free γ-CD, the Cu-γ-CD complex and a few peaks correspond to the Cu–SG complex, $(CD\text{-}GS\text{-}Cu\text{-}SG\text{-}CD\text{–}2H)^{2-}$ was also detected at high intensity. This can happen if the γ-CD–GSH inclusion complexes take part in Cu extraction. Two such inclusion complexes can bind to one Cu ion through the –S end. The other possibility could be that two GSH molecules first bind with one Cu ion, and the resulting complex then forms a 2:1 inclusion complex with γ-CD. Since the solution was stirred for 2 d before the ESI MS was performed, both possibilities exist. To confirm which could be the actual pathway of formation of such $(CD\text{-}GS\text{-}Cu\text{-}SG\text{-}CD\text{–}2\ H)^{2-}$ species, CID was performed where free $[\gamma\text{-}CD\text{–}H]^-$ and $[(GS\text{-}Cu\text{-}SG)\text{–}H]^-$ peaks were observed indicating that the second pathway is more likely to happen in the solution (Figure S10). Although the GS-Cu-SG complex would be more stable than the γ-CD–GSH inclusion complex considering ionic vs. non-covalent interactions, it is difficult to confirm the pathway of such complex formation. From previous studies[19] it is known that CD-GSH complexes are easy to synthesize and over

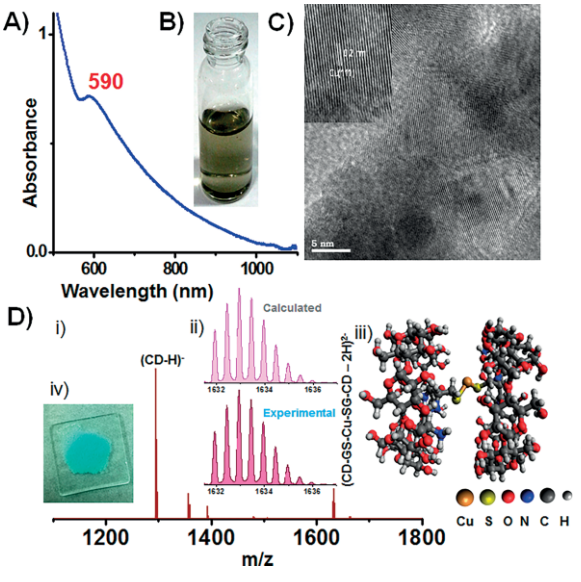

Figure 5. UV/Vis absorption spectra corresponding to the solution exposed to the copper vessel upon addition of ice-cold aqueous $NaBH_4$ solution. Cu nanoparticles were formed, which was confirmed by UV/Vis spectroscopy, exhibiting a characteristic peak at 590 nm. (B) Photograph of the colloid. (C) TEM images of the copper nanoparticles. (D) (i) ESI MS of the solution from a copper vessel containing GSH and γ-CD. (D) (ii) Theoretical and experimental mass spectra of an inclusion complex. (D) (iii) Schematic representation of the inclusion complex. (D) (iv) Photograph of the precipitated sample.

the timescale of 2 d such complexes can indeed form (Figure S11). One can imagine that the inclusion complex would have formed, which further stabilizes by binding with the extracted Cu ion. In both cases, GSH plays a significant role in the enhanced extraction and further stabilization of Cu in solution.

Conclusions

The research highlights the potential application of a green technology for an efficient extraction of noble metals by using inexpensive and environmentally benign reagents. Effective green extraction of silver and copper from metallic silver and copper by carbohydrates (γ-CD, glucose and β-CD) and synergistic enhancement of extraction in the presence of GSH and MBA are discussed. This synergistic effect in green extraction can contribute to new processes in extractive metallurgy of noble metals. A new cluster, $Ag_{20}(SG)_{15}CD^{3-}$, derived from the extracted ions, has been synthesized and characterized by spectroscopic and mass spectrometric techniques. Reacted silver foil was thoroughly studied by different techniques to obtain further insights into the mechanism. This study shows a new avenue for affordable noble metal extraction. A new approach for silver cluster synthesis would be of interest to the cluster community. Reacted silver foil showed unusual morphologies. We believe that the homogeneous Ag blade assemblies can be sensitive and cost-effective SERS substrates in molecular detection. Synergistic enhancement of extraction of precious metals may be extended to create greener processes.

Experimental Section

Chemicals and Materials: Silver foil (> 98 % purity), a copper vessel, silver vessel (98.5 % purity), brass vessel (60.66 % copper, 36.58 % zinc) and stainless steel plate (304 grade) were purchased from the local market. (+)-D-Glucose (G), β-CD, glutathione (GSH), *para*-mercaptobenzoic acid (MBA) and sodium borohydride ($NaBH_4$) were purchased from Sigma–Aldrich. γ-CD was purchased from TCI Japan. Deionized (DI) water was used throughout the experiments unless specified. Teflon beakers (250 mL) were procured from a local supplier.

Methods: A polished silver foil was immersed in a 250-mL teflon beaker containing cyclodextrin (60 mg) and GSH (200 mg) dissolved in DI water (200 mL) and heated at 70 °C for 7 d with constant stirring. Samples were collected at regular intervals for inductively coupled plasma mass spectrometry (ICP MS) and other analyses. A similar experimental procedure was carried out with MBA (50 mg and 75 mg) in place of GSH. Several control experiments were performed to obtain optimized conditions. For cluster synthesis, the desired amount of solution (see later) was collected and reduced with ice-cold aqueous $NaBH_4$ solution (1 M), and the as-formed cluster was characterized using UV/Vis spectroscopy and electrospray ionization mass spectrometry (ESI MS). After reaction, the foil was thoroughly characterized by scanning electron microscopy (SEM), transmission electron microscopy (TEM), Raman spectroscopy and powder X-ray diffraction (XRD). γ-CD/glucose (ca. 70 mg) was placed in silver, copper, brass and stainless steel vessels in DI water (70 mL). The reaction mixtures were kept at 65 °C while stirring for 7 d. Samples were collected at regular intervals for inductively coupled plasma mass spectrometry (ICP MS) and other analyses.

Instrumentation

ICP MS: ICP MS was performed using a Perkin–Elmer NexION 300X instrument equipped with Ar plasma. Before measuring any sample, the instrument was first calibrated with an Ag standard ($AgNO_3$) of five different concentrations (0, 10, 100, 1000 and 10000 ppb) to obtain a calibration curve with R^2 = 0.9999. A blank experiment (0 ppb) was performed with milliQ water (18.3 MΩ resistance) with 5 % (v/v) nitric acid. Standards were also prepared in 5 % nitric acid. The same amount (5 %) of nitric acid was added to the collected samples before analyses. For other metals, the instrument was calibrated with the standard by the same procedure.

ESI MS: ESI MS analyses of complexes (without $NaBH_4$ addition) were performed with an AB Sciex 3200 QTRAP LC MS/MS instrument over the range m/z = 100–1700 and Waters' Synapt G2Si HDMS instrument. The optimized conditions for QTRAP measurements were: ion spray voltage (ISV) 4 kV, declustering potential (DP) 60 V and entrance potential (EP) 10 V. The sample flow rate was kept at 5–10 μL/min. For tandem mass spectrometric analyses, the collision energy was varied from 10 to 100 (instrumental unit). All the data were collected in the positive mode and averaged for 100 spectra. All the γ-CD–metal complexes were analyzed by a Waters Synapt G2Si HDMS instrument. The optimized conditions for these measurements were as follows: flow rate 10–20 μL/min; capillary voltage 2–3 kV; cone voltage 120–150 V; source offset 80–120 V; desolvation gas flow 400 L/h. The as-formed silver thiolates in solution were converted into silver clusters after reduction with $NaBH_4$. The as-synthesized clusters were dissolved in 1:1 (v/v) water/MeOH and analyzed by a Thermo Scientific LTQ XL instrument over the range m/z = 100–4000. The optimized conditions used were as follows: source voltage 3 kV; sample flow rate 10 μL/min. The capillary temperature was varied from 120 to 270 °C.

ITC: Isothermal calorimetric experiments were performed using a GE Microcal ITC200. The instrument has two cells made of hastelloy with a 200 μL cell volume of which one is used for the sample and the other is used for the reference. The maximum volume that can be injected is 40 μL through a syringe with sub-micro litre precision.

Spectroscopy: UV/Vis absorption spectroscopic studies were performed with a Perkin–Elmer Lambda 25 instrument over the range 200–1100 nm with a band pass of 1 nm. Raman spectroscopic measurements were performed using a Witec GmbH, Alpha-SNOM alpha300 S confocal Raman instrument equipped with a 532 nm laser as the excitation source. High-resolution transmission electron microscopy (HRTEM) was performed with a JEOL 3010, 300 kV instrument equipped with a UHR polepiece. SEM and energy dispersive analysis of X-rays (EDS) were performed using a FEI QUANTA-200 SEM. The XRD analysis was performed using a Bruker D8 advance instrument equipped with Cu-K_α radiation source in the 2θ range of 5–90°.

Acknowledgments

We thank the Department of Science and Technology, Government of India for constantly supporting our research program on nanomaterials. A. N. and B. M. thank IIT Madras for doctoral fellowships. A. B. thanks IIT Madras for a postdoctoral fellowship. P. C. thanks the Council of Scientific and Industrial Research (CSIR) for her research fellowship. A. N. also thanks Mohd Azhardin Ganayee for the Raman measurements, Sandeep Bose for SEM measurements, Anil Kumar Avula for ICP MS measurements and Dr. Soumabha Bag for his help and suggestions.

Keywords: Green chemistry · Synergistic effect · Cluster compounds · Mass spectrometry · Blade-like structures · Silver

[1] J. Turkevich, P. C. Stevenson, J. Hillier, *Discuss. Faraday Soc.* **1951**, *11*, 55–75.

[2] a) J. P. Wilcoxon, B. L. Abrams, *Chem. Soc. Rev.* **2006**, *35*, 1162–1194; b) M. W. Heaven, A. Dass, P. S. White, K. M. Holt, R. W. Murray, *J. Am. Chem. Soc.* **2008**, *130*, 3754–3755; c) Z. Wu, E. Lanni, W. Chen, M. E. Bier, D. Ly, R. Jin, *J. Am. Chem. Soc.* **2009**, *131*, 16672–16674; d) K. M. Harkness, D. E. Cliffel, J. A. McLean, *Analyst* **2010**, *135*, 868–874; e) J. De Haeck, N. Veldeman, P. Claes, E. Janssens, M. Andersson, P. Lievens, *J. Phys. Chem. A* **2011**, *115*, 2103–2109; f) W. Wei, Y. Lu, W. Chen, S. Chen, *J. Am. Chem. Soc.* **2011**, *133*, 2060–2063; g) P. L. Xavier, K. Chaudhari, A. Baksi, T. Pradeep, *Nano Rev.* **2012**, *3*, 14767, https://doi.org/10.3402/nano.v3i0.14767; h) L. G. AbdulHalim, S. Ashraf, K. Katsiev, A. R. Kirmani, N. Kothalawala, D. H. Anjum, S. Abbas, A. Amassian, F. Stellacci, A. Dass, I. Hussain, O. M. Bakr, *J. Mater. Chem. A* **2013**, *1*, 10148–10154; i) H. Yang, J. Lei, B. Wu, Y. Wang, M. Zhou, A. Xia, L. Zheng, N. Zheng, *Chem. Commun.* **2013**, *49*, 300–302; j) H. Yang, Y. Wang, H. Huang, L. Gell, L. Lehtovaara, S. Malola, H. Häkkinen, N. Zheng, *Nat. Commun.* **2013**, *4*, 2422; k) J. Hassinen, P. Pulkkinen, E. Kalenius, T. Pradeep, H. Tenhu, H. Häkkinen, R. H. A. Ras, *J. Phys. Chem. Lett.* **2014**, *5*, 585–589; l) A. Mathew, T. Pradeep, *Part. Part. Syst. Charact.* **2014**, *31*, 1017–1053; m) Z. Wu, D.-e. Jiang, A. K. P. Mann, D. R. Mullins, Z.-A. Qiao, L. F. Allard, C. Zeng, R. Jin, S. H. Overbury, *J. Am. Chem. Soc.* **2014**, *136*, 6111–6122; n) R. Jin, C. Zeng, M. Zhou, Y. Chen, *Chem. Rev.* **2016**, *116*, 10346–10413.

[3] a) M. Walter, J. Akola, O. Lopez-Acevedo, P. D. Jadzinsky, G. Calero, C. J. Ackerson, R. L. Whetten, H. Grönbeck, H. Häkkinen, *Proc. Natl. Acad. Sci. USA* **2008**, *105*, 9157–9162; b) M. Zhu, C. M. Aikens, F. J. Hollander, G. C. Schatz, R. Jin, *J. Am. Chem. Soc.* **2008**, *130*, 5883–5885; c) X. Yuan, Z. Luo, Q. Zhang, X. Zhang, Y. Zheng, J. Y. Lee, J. Xie, *ACS Nano* **2011**, *5*, 8800–8808; d) C. Zeng, H. Qian, T. Li, G. Li, N. L. Rosi, B. Yoon, R. N. Barnett, R. L. Whetten, U. Landman, R. Jin, *Angew. Chem. Int. Ed.* **2012**, *51*, 13114–13118; *Angew. Chem.* **2012**, *124*, 13291; e) M. Zhou, S. Dagan, V. H. Wysocki, *Angew. Chem. Int. Ed.* **2012**, *51*, 4336–4339; *Angew. Chem.* **2012**, *124*, 4412; f) M. Zhou, C. Huang, V. H. Wysocki, *Anal. Chem.* **2012**, *84*, 6016–6023; g) T. Zhou, M. Rong, Z. Cai, C. J. Yang, X. Chen, *Nanoscale* **2012**, *4*, 4103–4106; h) T. Udayabhaskararao, T. Pradeep, *J. Phys. Chem. Lett.* **2013**, *4*, 1553–1564; i) H. Yang, Y. Wang, N. Zheng, *Nanoscale* **2013**, *5*, 2674–2677; j) Y. Yu, X. Chen, Q. Yao, Y. Yu, N. Yan, J. Xie, *Chem. Mater.* **2013**, *25*, 946–952; k) X. Yuan, M. I. Setyawati, A. S. Tan, C. N. Ong, D. T. Leong, J. Xie, *NPG Asia Mater.* **2013**, *5*, e39; l) J. Zhang, X. Wang, Y. Fu, Y. Han, J. Cheng, Y. Zhang, W. Li, *Langmuir* **2013**, *29*, 14345–14350; m) T.-y. Zhou, L.-p. Lin, M.-c. Rong, Y.-q. Jiang, X. Chen, *Anal. Chem.* **2013**, *85*, 9839–9844; n) H. Yang, Y. Wang, J. Yan, X. Chen, X. Zhang, H. Häkkinen, N. Zheng, *J. Am. Chem. Soc.* **2014**, *136*, 7197–7200; o) M. Zhou, V. H. Wysocki, *Acc. Chem. Res.* **2014**, *47*, 1010–1018; p) C. P. Joshi, M. S. Bootharaju, M. J. Alhilaly, O. M. Bakr, *J. Am. Chem. Soc.* **2015**, *137*, 11578–11581.

[4] T. D. Veenstra, *Biophys. Chem.* **1999**, *79*, 63–79.

[5] a) Z. Liu, M. Frasconi, J. Lei, Z. J. Brown, Z. Zhu, D. Cao, J. Iehl, G. Liu, A. C. Fahrenbach, Y. Y. Botros, O. K. Farha, J. T. Hupp, C. A. Mirkin, J. Fraser Stoddart, *Nat. Commun.* **2013**, *4*, 1855; b) Z. Liu, A. Samanta, J. Lei, J. Sun, Y. Wang, J. F. Stoddart, *J. Am. Chem. Soc.* **2016**, *138*, 11643–11653.

[6] Y. Liu, K. Ai, X. Cheng, L. Huo, L. Lu, *Adv. Funct. Mater.* **2010**, *20*, 951–956.

[7] M. Sastry, A. Ahmad, M. Islam Khan, R. Kumar, *Curr. Sci.* **2003**, *85*, 162–170.

[8] a) S. Cherevko, A. R. Zeradjanin, A. A. Topalov, N. Kulyk, I. Katsounaros, K. J. J. Mayrhofer, *ChemCatChem* **2014**, *6*, 2219–2223; b) N. Hodnik, C. Baldizzone, G. Polymeros, S. Geiger, J.-P. Grote, S. Cherevko, A. Mingers, A. Zeradjanin, K. J. J. Mayrhofer, *Nat. Commun.* **2016**, *7*, 13164; c) A. I. Yanson, P. Rodriguez, N. Garcia-Araez, R. V. Mom, F. D. Tichelaar, M. T. M. Koper, *Angew. Chem. Int. Ed.* **2011**, *50*, 6346–6350; *Angew. Chem.* **2011**, *123*, 6470.

[9] A. Baksi, M. Gandi, S. Chaudhari, S. Bag, S. S. Gupta, T. Pradeep, *Angew. Chem. Int. Ed.* **2016**, *55*, 7777–7781; *Angew. Chem.* **2016**, *128*, 7908.

[10] a) Y. Negishi, K. Nobusada, T. Tsukuda, *J. Am. Chem. Soc.* **2005**, *127*, 5261–5270; b) S. Kumar, M. D. Bolan, T. P. Bigioni, *J. Am. Coal Soc.* **2010**, *132*, 13141–13143; c) A. Ghosh, T. Udayabhaskararao, T. Pradeep, *J. Phys. Chem. Lett.* **2012**, *3*, 1997–2002.

[11] A. A. Bagabas, M. Frasconi, J. Iehl, B. Hauser, O. K. Farha, J. T. Hupp, K. J. Hartlieb, Y. Y. Botros, J. F. Stoddart, *Inorg. Chem.* **2013**, *52*, 2854–2861.

[12] T. Udayabhaskararao, M. S. Bootharaju, T. Pradeep, *Nanoscale* **2013**, *5*, 9404–9411.

[13] A. Baksi, M. S. Bootharaju, X. Chen, H. Häkkinen, T. Pradeep, *J. Phys. Chem. C* **2014**, *118*, 21722–21729.

[14] A. Mathew, G. Natarajan, L. Lehtovaara, H. Häkkinen, R. M. Kumar, V. Subramanian, A. Jaleel, T. Pradeep, *ACS Nano* **2014**, *8*, 139–152.

[15] W. Qian, S. Krimm, *Biopolymers* **1994**, *34*, 1377–1394.

[16] P. D. Jadzinsky, G. Calero, C. J. Ackerson, D. A. Bushnell, R. D. Kornberg, *Science* **2007**, *318*, 430–433.

[17] S. E. Hunyadi, C. J. Murphy, *J. Mater. Chem.* **2006**, *16*, 3929–3935.

[18] a) S. Zong, Z. Wang, H. Chen, J. Yang, Y. Cui, *Anal. Chem.* **2013**, *85*, 2223–2230; b) Q. Zhang, X. Lu, P. Tang, D. Zhang, J. Tian, L. Zhong, *Plasmonics* **2016**, *11*, 1361–1368.

[19] M. Garcia-Fuentes, A. Trapani, M. J. Alonso, *Eur. J. Pharm. Biopharm.* **2006**, *64*, 146–153.

Received: February 20, 2017